EFFECTS OF INLET CONDITIONS ON SKEWED AND PITCHED JETS IN CROSS-FLOW

James P. Johnston
and
Bruce P. Mosier
Stanford University
Department of Mechanical Engineering
Stanford, CA 94305-3030, USA
jpj@stanford.edu

Zia U. Khan
A.T. Kearney
153 East 53rd Street
New York, NY 10022, USA

ABSTRACT

An experimental study of flow downstream of round, pitched and skewed wall-jets (vortex generating jets) is presented to illustrate the effects of changing the geometric inlet conditions of the jet-holes. In one case the jet-hole has a smoothly-contoured inlet, and in the other the inlet was a sharp-edged , sudden contraction. The test region geometry, mean jet flow and cross-flow conditions were otherwise identical.

In both cases, dominant streamwise vortex structures are seen in the boundary layer downstream; the flow and turbulence is nearly the same in the far-field starting at a location where x/D > 5. In the near-field, for x/D < 5, there are significant differences; turbulence levels are higher, and the start of the dominant vortex shape is less clear for the sharp-edged case. This is believed to be the result of flow separation and free shear layer instability inside the jet-hole which is not present for the smoothly-contoured case.

INTRODUCTION

Vortex-generating wall jets may be used (i) to mix low-momentum boundary-layer fluid with high-momentum freestream fluid for the suppression of flow separation, Johnston and Nishi (1990), or (ii) for film cooling of gas turbine blades using cross-compound injection of compressed air, Honami, et al. (1994). However, modification of geometry at the jet-hole inlet may have substantial effects on mean flow and turbulence development downstream of jet injection; effects that may be important in both applications.

Jets in cross-flow with various velocity ratios (jet speed / cross-flow speed) were studied experimentally at several downstream planes. The jet-holes were pitched up from the wall at 30°, and skewed relative to the cross-flow direction (x-axis) by 60°. Detailed measurements of mean velocity, mean streamwise vorticity, and the six Reynold's stresses were obtained with a three-component laser-Doppler velocimetry (LDV) system used in previous studies.

Here, two round (D = 25.4 mm) jet-hole configurations were employed, see Figure 1. The flow fields that result from the jet-hole which is proceeded upstream by a *smoothly-contoured* inlet nozzle were studied by Khan and Johnston (1999, 2000). This configuration created a flow in the jet-hole which was nearly uniform except for the thin boundary layers on the inside of the hole. In the second configuration, flow entered the *sharp-edged* hole at very low speed from a large plenum chamber, and, as a result, was severely separated over the sharp edge on the downstream side of the hole. The resulting changes in velocity profile and turbulence in the jet flow which emerges from the sharp-edged hole into the cross-flow were expected to change the flow structure downstream, in particular the dominant streamwise vortex, but the extent of the changes and the degree of the effects that would occur were unknown.

Compton & Johnston (1990) and Khan & Johnston (1999) using smoothly-contoured jet-holes showed that a skew of 60° appeared to be the geometry that maximized the strength of the dominant vortex. With this in mind, 60° was chosen for the sharp-edged hole, a geometry more likely to be used in practice than the complex smoothly-contoured geometry.

We anticipated that the additional turbulence and dissipation generated as a result of local flow separation over the sharp-edged inlet and the *vena-contracta* effect in the hole could have substantial consequences, the most important being a more rapid dissipation of the dominant vortex which extends downstream near the wall. Flow

visualization and LDV data of the resulting jet structure from the jet exit plane up to x/D = 5 (end of near-field region) showed that the change of the jet inlet geometry had substantial effects which are described below. However, surprisingly, the measured velocity, vorticity, and turbulence statistics in the far-field region, at x/D = 10 and 20, produced nearly identical results for both inlets.

The possible consequences of these results are different, depending on the application: (i) In the case of vortex generating jets (VGJs) for separation control the use of a smoothly-contoured inlet would appear to have little value because the strength of the dominant vortex, the principle cross-stream mixing mechanism is unchanged in the far-field. (ii) On the other hand, for film cooling with cross-compound injection, the higher turbulence levels in the region near the hole in the case of the sharp-edged hole might increase local heat transfer rates and decrease cooling effectiveness, which points to a potential benefit if smoothly-contoured film cooling holes could be used.

EXPERIMENTAL PROCEDURE

The experiments were conducted in a low-speed water channel with a single jet plug inserted at the center of a flat wall on which a two-dimensional boundary layer grew. The *cross-flow* and the *mean jet* speeds (U_e and V_{jet}) were both set at 20 cm/s for the LDV measurements, and both were near 5 cm/s for flow visualization. Conditions and measurement techniques were the same as described in Khan and Johnston (1999). All quatitative results are reported in dimensionless form based on the cross-flow free stream speed U_e and the jet-hole diameter, D (2.54 cm).

LDV data were taken in planes perpendicular to the wall at 5, 10, and 20 jet-hole diameters downstream. At each plane, profiles from the wall to the freestream were obtained at a number of spanwise locations for each data plane. With the jet flow off, the test surface boundary layer was two-dimensional and turbulent, with a momentum thickness Reynolds number of 1100 and a thickness of about 2D. In the results, it is seen that the jet flow severely perturbs the spanwise two-dimensionality.

Flow visualization, using fluorescein dissolved in water and an argon-ion Laser sheet, was performed in the same manner as described in Khan and Johnston (1999). The dyed fluid was mixed into the jet fluid well upstream of the inlet to the jet-hole. No boundary layer trip was present on the shortened cross-flow wall. Thus, a thin, laminar boundary layer was present at the location of the jet-hole. Video images were acquired at several planes perpendicular to the main channel flow.

EXPERIMENTAL RESULTS

Flow visualization of the jet fluid for both the sharp-edge inlet and for the smoothly-contoured inlet, at several downstream positions near the center of the jet-hole, were included in video studies of the near-field. Several individual video frames for both cases are shown in Figure 2. The flow is very unsteady in the sharp-edge case and thus no individual fame is truly representative.

In summary, the overall flow structure of the sharp-edge jet is similar to that of the smooth-inlet jet in that both appear to contain a dominant vortex (right hand side of each frame). The general circulation associated with the dominant vortex is not always clear in single frames, but may be more easily discerned by watching the video. In contrast to the smoothly-contoured case where the flow is relatively steady, the video shows substantially more unsteadiness in the sharp-edge case. It is likely that the origin of this enhanced unsteadiness lies inside the jet-hole. In contrast with the smoothly contoured jet, the flow in the sharp-edge case separates at the sharp edge as it enters the jet-hole and creates a free shear layer downstream. We believe that the Kelvin-Helmholtz instability of this free shear layer enhances the unsteadiness of the flow in the jet.

The quantitative mean velocity data are compared in Figures 3 and 4. They show the general circulation patterns of the dominant vortex in the far-field, at x/D = 10 and 20. The circulation in the y-z plane (secondary flow) is indicated by the V+W vectors which are overlaid on the U coutour lines. All velocities are normalized on the freestream speed. Close to the hole exit, at x/D = 5, the clear existence of a well-developed vortex core is questionable, especially for the sharp-edged case. Further downstream, at x/D = 10 and 20, the low speed, wall boundary layer eventually ends up in the core region as evidenced by the low values of streamwise velocity (U = 0.75) on closed contours close to the center of secondary circulation.

These observations were augmented by study of contours of mean streamwise vorticity (computed from the mean secondary velocities, V and W). Here, a region that might be called the core of the dominant vortex is seen at x/D = 5, but the contour lines outside the core are far from the circular to oval shapes expected for the dominant vortex, especially in the sharp-edged case. Table 1 shows the peak magniture of vorticity in the core region at x/D = 5, 10, and 20. The rate of decay of streamwise vorticity with downstream distance is strongest upstream of x/D = 10 for the sharp-edged jet-hole, but about the same for both cases downstream of x/D = 10, in the far-field.

The quantitative data at x/D = 5, 10, and 20 for the turbulent kinetic energy (actually, $q^2 = 2$ K) are shown side-by-side in Figures 5 (sharp-edged) and 6 (smoothly-contoured). The vectors shown on the plots represent the transport of q^2 by the turbulence itself in the plane of data. The most interesting feature of these results is seen when the cases are compared at x/D = 5, the downstream end of the

near-field. The jet-hole with the sharp-edged inlet produced almost double the turbulent kinetic energy as the smoothly-contoured case. However, at the downstream stations (x/D = 10 and 20), the turbulence is only slightly higher for the sharp-edged case.

The high, initial turbulence level is thought to originate in the instability and unsteadiness of the thin shear-layer formed by separation at the inlet to the sharp-edged jet-hole (see discussion in Conclusions, below). This intense shear-layer turbulence occurs on a smaller scale than the turbulence generated later due to the jet/cross-flow interaction outside of the hole, and hence appears to decay rapidly downstream as indicated in Table 2 which gives q^2 values in the dominant vortex core at x/D = 5, 10, 20.

CONCLUSIONS

The near-field region, x/D<5, is substantially influenced by the inlet geometry of the jet-hole. Sharp edges over which inlet flow can separate create a stalled region inside the hole. Area blockage by the low-speed stalled region narrows and accelerates the jet core flow so that it is faster than the mean jet speed (based on hole cross sectional area). A thin shear layer exists along the edge of the separated jet, inside the hole. This shear layer is unstable and its unsteadiness is believed to be the source of intense turbulence not observed in the near field of the smoothly-contoured case where no flow separation occurs inside the jet-hole. Eventually, downstream in the far-field, the effects of initial conditions damp out and the strength and decay rate of the dominant streamwise vortex depends only on gross hole geometry: pitch and skew angle, and the ratio of mean jet speed to cross-flow speed.

References

Compton, D.A. and Johnston, J.P., 1992, "Streamwise Vortex Production by Pitched and Skewed Jets in a Turbulent Boundary Layer," AIAA Journal, Vol. 30, pp. 640-647.

Honami, S., Shizawa, T., and Uchiyama, A., 1994, "Behavior of the laterally injected jet in film cooling: measurements of surface temperature and velocity/temperature field within the jet," ASME *Journal of Turbomachinery*, Vol. 116, pp. 106-112.

Johnston, J.P. and Nishi, M., 1990, "Vortex generator jets – means for flow separation control," AIAA Journal, Vol. 28, pp. 429-436.

Khan, Z.U. and Johnston, J.P., 1999, "On the Dominant Vortex Created by a Pitched and Skewed Jet in Crossflow," Report TSD-122, Mech. Engr. D., Stanford U., March 1999.

Khan, Z.U. and Johnston, J.P., 2000, "On Vortex Generating Jets," *International Journal of Heat and Fluid flow*, Vol. 21, pp. 506-511.

TABLES

x/D	Sharp-edge	Smooth-contour
5.0	2.79	1.60
10.0	0.97	0.90
20.0	0.57	0.45

Table 1 : Magnitude of mean streamwise vorticiy in the dominant vortex core for two jet-hole inlet shapes.

x/D	Sharp-edge	Smooth-contour
5.0	0.240	0.085
10.0	0.040	0.040
20.0	0.020	0.018

Table 2 : q^2, 2 x turbulence kinetic energy in the dominant vortex core for two jet-hole inlet shapes.

Figures

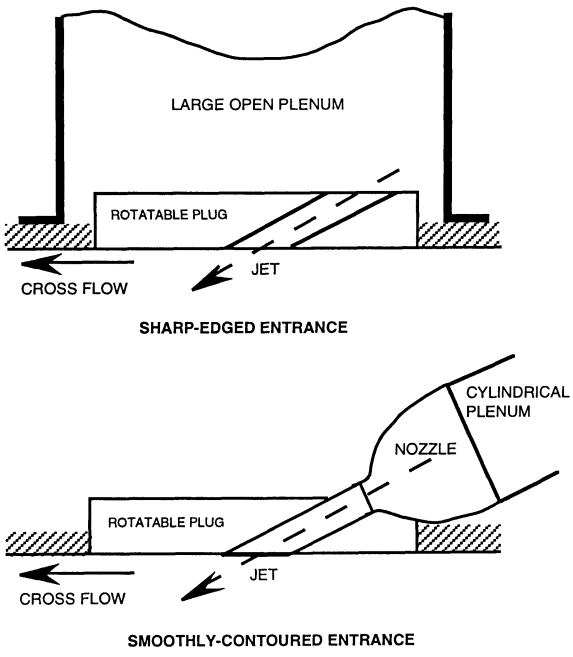

Figure 1 : Two jet-hole configurations (see Figure 2 in Khan and Johnston (2000) for more detail.) Note that the pitch angle of the holes was 30 degrees from the plane of the wall and the jet-hole was skewed at 60 degrees from the downstream direction of the cross-flow. Hole: diameter, D = 25.4 mm; length, L = 88.4 mm.

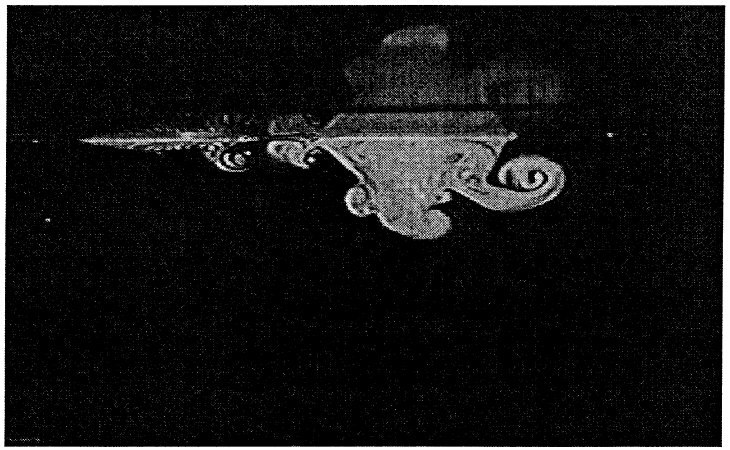

Sharp-edged jet-hole - x/D = 0.72

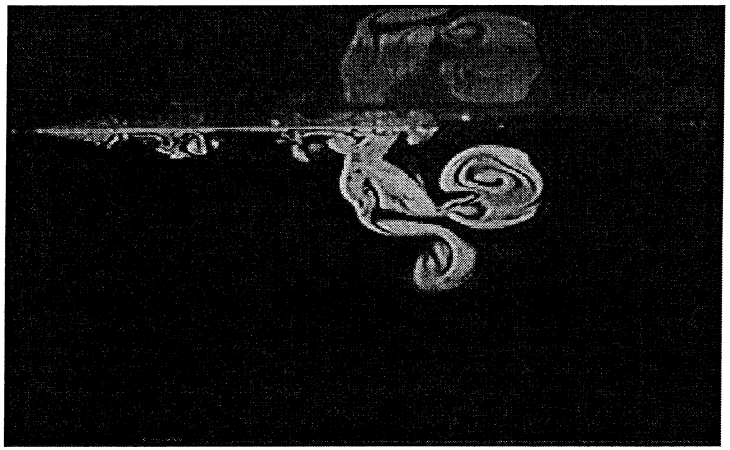

Sharp-edged jet-hole - x/D = 2.0

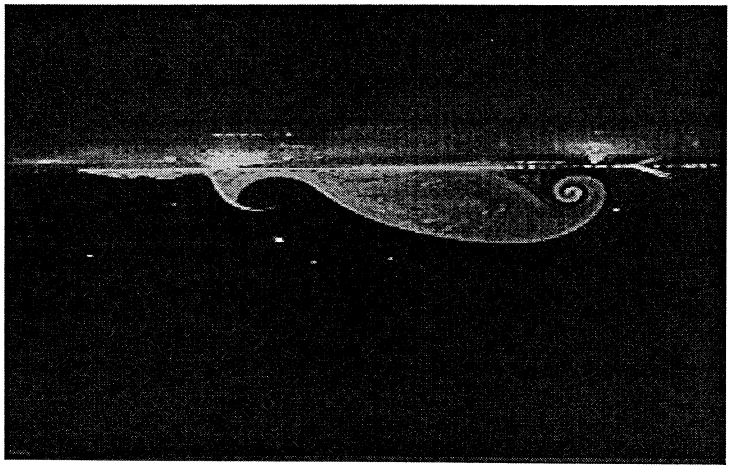

Smoothly-contoured jet-hole - x/D = 0.72

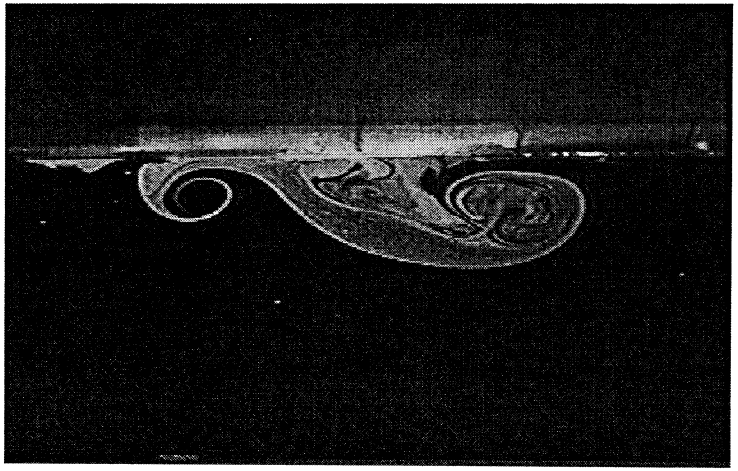

Smoothly-contoured jet-hole - x/D = 2.0

Figure 2 : Jet structure in dyed jet fluid illuminated normal to cross-flow by thin plane of laser light at two positions in the near-field, just downstream of the center of the exit of the jet-hole. The reflection of the image in the smooth wall is seen at the top of each photo. Jet-hole pitch = 30°, skew = 60°, and U_e/V_{jet} = 1.0 (jet speed and freestream speed of 5 cm/sec) in water channel for all cases.

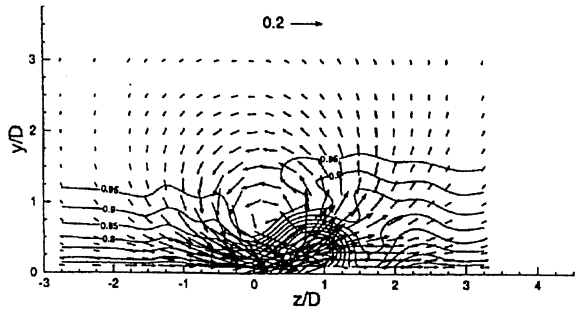

(a) $x/D = 5$

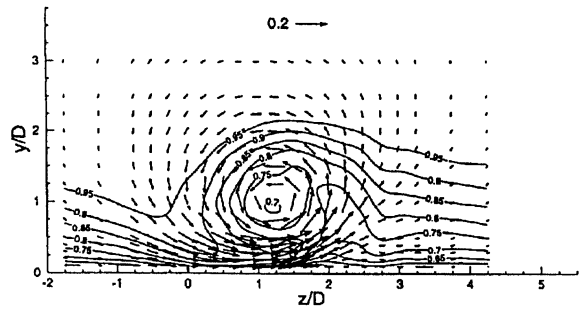

(b) $x/D = 10$

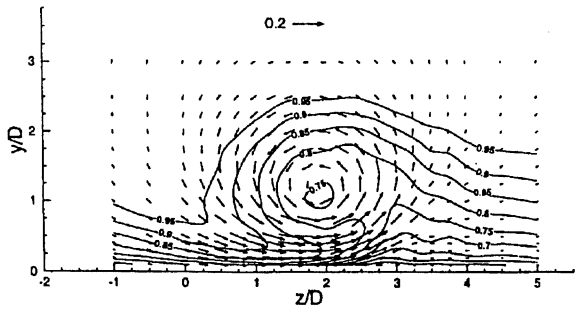

(c) $x/D = 20$

Figure 3 : Sharp-edge jet-hole - Contours of mean streamwise velocity, U, with secondary flow (V+W) vectors superposed at three downstream stations. Outer contour is set at U/Ue = 0.95, central contour = 0.7 for x/D = 10 and 0.75 for x/D = 20. Secondary vector of 0.2 U_e shown for reference.

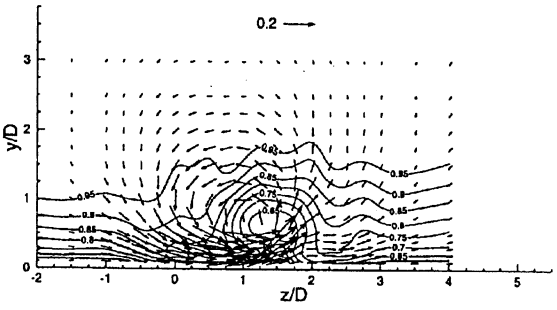

(a) $x/D = 5$

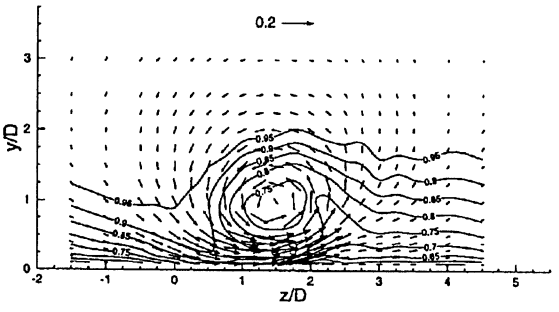

(b) $x/D = 10$

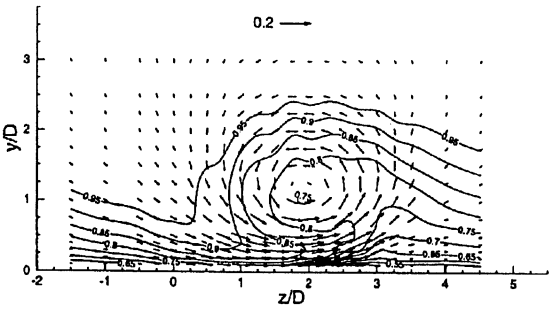

(c) $x/D = 20$

Figure 4 : Smoothly-contoured jet-hole - Contours of mean streamwise velocity, U, with secondary flow (V+W) vectors superposed at three downstream stations. Outer contour is set at U/Ue = 0.95, central contour = 0.8 for x/D = 5 and 0.75 for x/D = 10 and 20. Secondary vector of 0.2 U_e shown for reference.

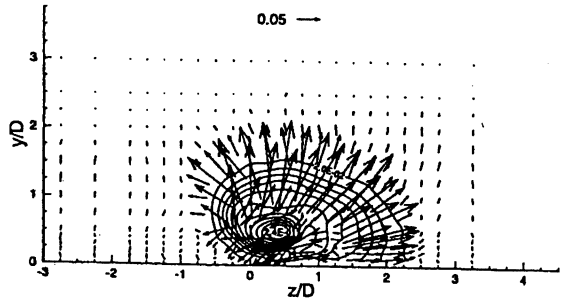

(a) $x/D = 5$

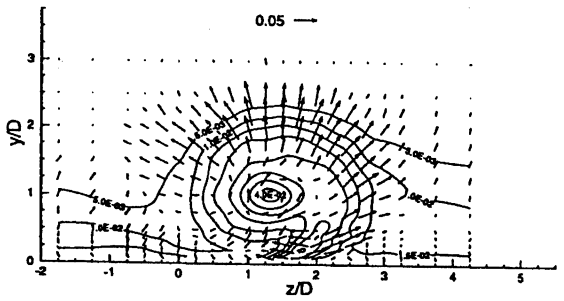

(b) $x/D = 10$

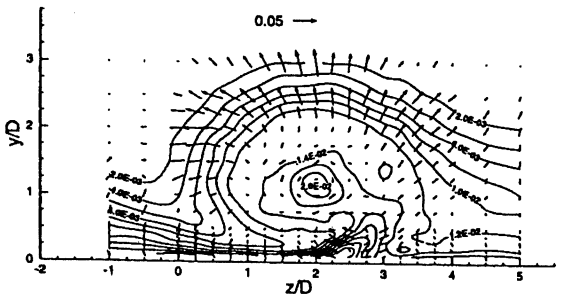

(c) $x/D = 20$

Figure 5 : Sharp-edge jet-hole - Contours of q^2 (2 x turbulent kinetic energy) normalized on U_e^2. Vectors represent transport of q^2 by turbulence velocity (v and w) in y-z plane. Max/min contour values are 0.24/0.02 at x/D = 5; 0.04/0.005 at x/D = 10; 0.02/0.002 at x/D = 20.

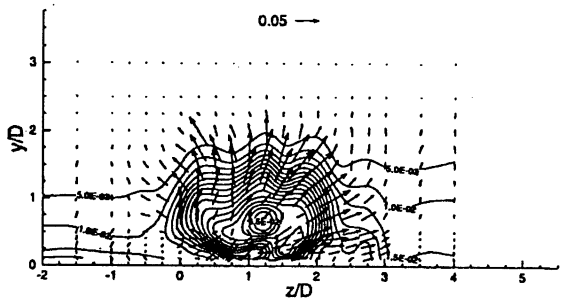

(a) $x/D = 5$

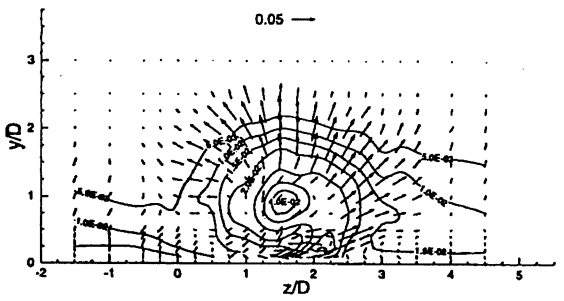

(b) $x/D = 10$

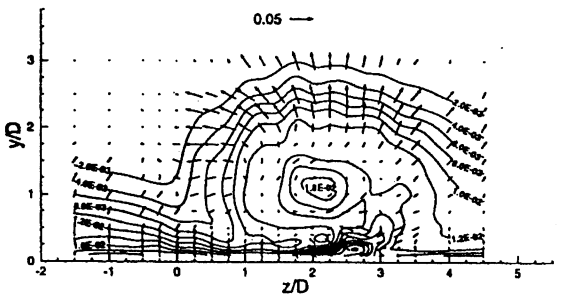

(c) $x/D = 20$

Figure 6 : Smoothly-contoured jet-hole - Contours of q^2 (2 x turbulent kinetic energy) normalized on U_e^2. Vectors represent transport of q^2 by turbulence velocity (v and w) in y-z plane. Max/min contour values are 0.085/0.005 at x/D = 5; 0.04/0.005 at x/D = 10; 0.02/0.0018 at x/D = 20.